Biosensors and Bioelectronics 26 (2010) 1736–1742

Contents lists available at ScienceDirect

Biosensors and Bioelectronics

journal homepage: www.elsevier.com/locate/bios

Short communication

A multiplex nanoparticle-based bio-barcoded DNA sensor for the simultaneous detection of multiple pathogens☆

Deng Zhang, Michael C. Huarng, Evangelyn C. Alocilja*

Department of Biosystems and Agricultural Engineering, Michigan State University, East Lansing, MI 48824, United States

ARTICLE INFO

Article history:
Received 15 April 2010
Received in revised form 16 July 2010
Accepted 4 August 2010
Available online 11 August 2010

Keywords:
Biosensor
Bio-barcode DNA
DNA probe
Screen-printed carbon electrode

ABSTRACT

A highly amplified, nanoparticle-based, bio-barcoded electrochemical biosensor for the simultaneous multiple detection of the protective antigen A (*pagA*) gene (accession number, M22589) of *Bacillus anthracis* and the insertion element (*Iel*) gene (accession number, Z83734) of *Salmonella enteritidis* is reported in this paper. The biosensor system is mainly composed of three nanoparticles: gold nanoparticles (AuNPs), magnetic nanoparticles (MNPs), and nanoparticle tracers (NTs, such as PbS and CdS). The AuNPs are coated with the first target-specific DNA probe (1pDNA), which can recognize one end of the target DNA sequence (tDNA), and many NT-terminated bio-barcode ssDNA (bDNA-NT), which act as signal reporter and amplifier. The MNPs are coated with the second target-specific DNA probe (2pDNA) that can recognize the other end of the target gene. After binding the nanoparticles with the target DNA, the following sandwich structure is formed: MNP-2pDNA/tDNA/1pDNA-AuNP-bDNA-NTs. A magnetic field is applied to separate the sandwich structure from the unreacted materials. Because the AuNPs have a large number of nanoparticle tracers per DNA probe binding event, there is substantial amplification. After the nanoparticle tracer is dissolved in 1 M nitric acid, the NT^{2+} ions are detected by square wave anodic stripping voltammetry (SWASV) on screen-printed carbon electrode (SPCE) chips. The results show that the detection limit of this multiplex bio-barcoded DNA sensor are 0.5 ng/mL of the insertion element (*Iel*) gene of *S. enteritidis* using CdS, and 50 pg/mL of the *pagA* gene of *B. anthracis* using PbS NTs. The nanoparticle-based bio-barcoded DNA sensor has potential application in rapid detection of multiple pathogenic agents in the same sample.

1. Introduction

The development of systems allowing rapid DNA detection is motivated by applications in many fields: DNA diagnostics, gene analysis, fast detection of biological warfare agents, and forensic applications (Sassolas et al., 2008). DNA sensor usually relies on the immobilization of a single-stranded DNA (ssDNA) probe onto a surface to recognize its complementary DNA target sequence by hybridization. Transduction of hybridization of DNA can be measured electronically (Ricci et al., 2009), optically (Dubertret, 2005; Pu et al., 2008; Sassolas et al., 2008), electrochemically (Drummond et al., 2003; Weng et al., 2008), or using mass-sensitive devices (Huang et al., 2006). Although optical detection method for barcode DNA (bDNA) is commonly used and current optical sensing approaches are effective for high-density arrays, they are hard to miniaturize and use for in-field detection or diagnosis. Electrochemical systems for biomedical diagnostics can be miniaturized and integrated into micro-systems, including parts for signal processing, providing great deal of advantages over optical detection (Templin et al., 2002). Indeed, portable systems for clinical testing and on-site environmental monitoring are now being developed (Wang, 2002). The basic categories of electrochemical detection of DNA include direct reduction/oxidation of DNA (Karadeniz et al., 2003; Ozkan-Ariksoysal et al., 2008), indirect oxidation of target DNA (tDNA) through the use of electrochemical mediators (Yang and Thorp, 2001), DNA-specific redox indicator detection (Miroslav Fojta, 2003), and DNA-mediated charge transport electrochemistry (Jackson and Hill, 2001; Steel et al., 1998).

Use of nanomaterials or nanoparticles in biosensors allows the use of many new signal transduction technologies. Many biosensors based on nanotechnology for the molecular detection of foodborne pathogens and bio-terrorism agents can be found in the literature. These detection techniques include conductive polymer nanowires (Pal et al., 2008), nano-porous silicon (Mathew and Alocilja, 2005; Zhang and Alocilja, 2008), gold nanoparticles (Li et al., 2009; Wang et al., 2010) and carbon nanotubes (Poonam and Deo, 2008). Three nanoparticle tracers (NTs) have been used to differentiate the signal of three DNA targets in connection with a sandwich hybridization assay and stripping voltammetry of the corresponding heavy metals (Wang et al.,

☆ Finalist for the World Congress on Biosensors 2010 selected Keynote Paper.

* Corresponding author. Tel.: +1 517 355 0083; fax: +1 517 432 2892.
E-mail address: alocilja@msu.edu (E.C. Alocilja).

0956-5663/$ – see front matter © 2010 Elsevier B.V. All rights reserved.
doi:10.1016/j.bios.2010.08.012

2003). A bio-barcoded DNA assay utilizes oligonucleotide-modified gold nanoparticles (AuNPs) for signal amplification and magnetic nanoparticles (MNPs) for easy separation from the sample. The large bDNA-to-recognition agent ratio provides a means of substantial signal amplification. It is promising as it allows the rapid detection of multiple protein targets at low-attomolar concentrations (Goluch et al., 2006) and nucleic acids at high-zeptomolar levels under optimized conditions (Nam et al., 2004).

In this paper, we describe a combination of the NT and bio-barcode approaches for a highly amplified, nanoparticle-based, bio-barcoded electrochemical biosensor. The biosensor is designed for the rapid detection of *pagA* gene of *Bacillus anthracis* (a well-known bio-terrorism agent) and insertion element (*Iel*) gene from *Salmonella enteritidis* (one of the most common foodborne pathogens). The biosensor utilizes nanoparticle tracers (NTs) terminating the ssDNA bio-barcode conjugated to the gold nanoparticles (AuNPs) as electrochemical indicators, and magnetic nanoparticles (MNPs) for easy and clean separation from the sample. After hybridization with the target DNA (tDNA), a magnetic field is used to separate the sandwich complex consisting of MNP-2pDNA/tDNA/1pDNA-AuNP-bDNA-NT. After the NTs (PbS and CdS) are dissolved in 1 M nitric acid, NT^{2+} ions (Pb^{2+} and Cd^{2+}) are measured by square wave anodic stripping voltammetry (SWASV) on a screen-printed carbon electrode (SPCE) chip and yield well-resolved highly sensitive stripping voltammetric signals for the corresponding targets. The new strategy combines multiple pathogen detection, magnetic extraction and concentration, and inherently amplified signal from the NT-bio-barcode assay.

2. Experimental

2.1. Reagents and materials

Hydrogen tetrachloroaurate (III) trihydrate and sodium citrate dehydrate were used for the synthesis of gold nanoparticles. Sodium sulfide, 3-mercaptoacetic acid, lead nitrate and cadmium chloride were used for the synthesis of lead sulfide (PbS) and cadmium sulfide (CdS) NTs. 1,4-Dithio-DL-threitol (DTT) was used for the cleavage of oxidized thiolated oligonucleotides. 1-Ethyl-3-[3-dimethylaminopropyl] carbodiimide hydrochloride (EDC) and N-hydroxysuccinimide (NHS) were used for the conjugation of carboxylic group on NTs and amine group on bio-barcoded AuNPs. Amine terminated MNPs were used for sample separation. All reagents were purchased from Sigma (St. Louis, MO). DNA isolation was performed using the QiaAmp DNA Mini Kit (Qiagen Inc., Valencia). Nap-5 column (GE Healthcare, Piscataway, NJ) was used to purify the DNA product from DTT solution. Sulfosuccinimidyl 4-N-maleimidomethyl cyclohexane-1-carboxylate (sulfo-SMCC, Pierce, WI) was used as a cross-linker between thiolated DNA probe (pDNA) and amine-coated MNPs. Sulfo-NHS acetate (Pierce, WI) was used to block unreacted sulfo-SMCC. Bismuth standard stock solution (1000 mg/L, atomic absorption standard solution) was obtained from Fisher Scientific (Hanover Park, IL, USA). All solutions were prepared in deionized water (~18 MΩ cm).

2.2. Apparatus

Target DNA (tDNA) was amplified by a thermocycler (Mastercycler Personal, Eppendorf). Gel electrophoresis (Runone System) was used to confirm the PCR product. After purification of the PCR product, a spectrophotometer (SmartSpec 3000, Bio-Rad Laboratories) was used to measure the concentration of pDNA in solution and tDNA in the sample. A transmission electron microscope (TEM, JEOL100 CXII) was used to image and characterize the NTs and AuNPs. All magnetic separation was done using a magnetic separator (FlexiMag, SpheroTech). A centrifuge (Micro12, Fisher Scientific) was used to separate and purify the nanoparticles. An incubator (HS-101, Amerex Instrument Inc.) was used for the hybridization reaction. Electrochemical measurement was performed with a potentiostat/galvanostat (263A, Princeton Applied Research, MA) that is connected to a personal computer. The electrochemical software operating system (PowerSuite, Princeton Applied Research, MA) was used for electrochemical measurement and data analysis. The integrated SPCE chips were purchased from Gwent Inc. England. A SPCE chip is composed of two electrodes: carbon electrode (working electrode), and silver/silver chloride electrode (counter and reference electrode). The working area is limited by a meshed well. The volume capacity of the electrochemical cell is 100 μL.

2.3. Bacteria culture, DNA isolation and PCR

S. enteritidis (strain S-64) and *B. anthracis* Sterne strain were grown following standard microbiological cultures. DNA isolation was performed using the QiaAmp DNA Mini Kit (Qiagen, Valencia, CA). Primers were designed for the detection of *S. enteritidis* using the insertion element (*Iel*) gene (Wang and Yeh, 2002). The single stranded forward and reverse primers were *Iel*L-5′-CTAACAGGCGCATACGATCTGACA-3′ and *Iel*R-5′-TACGCATAGCGATCTCCTTCGTT G-3′. The following thiolated oligonucleotides were used to conjugate with the nanoparticles: the first DNA probe (1pDNA) on AuNPs: 5′-AATATGCTGCCTACTGCCCTACGCTT-SH-3′; the second DNA probe (2pDNA) on MNPs: 5′-SH-TTTATGTAGTCCTGTATCTTCGCCGT-3′. The primers and pDNAs of the *pagA* gene (accession number, M22589) from *B. anthracis* Sterne strain were as follows: *pagA*L: 5′-AAAATGGAAGAGTGAGGGTG-3′; *pagA*R: 5′-CCGCCTTT-CTACCAGATTTA-3′; 1pDNA: 5′-SH-GGAAGAGTGAGGGTGGAT ACAGGCT-3′; 2pDNA: 5′-AGATTTAAATC TGGTAGAAAGGCGG–SH-3′ (Hill and Mirkin, 2006; Song et al., 2005); bDNA on AuNPs for both gene detection: 5′-NH_2-TTATTCGTAGCTAAAA AAAAAA-SH-3′ (Hill and Mirkin, 2006). All oligonucleotides were synthesized by the Integrated DNA Technologies Inc. (Coralville, IA). The PCR products were identified by gel electrophoresis and a UV transilluminator after purification. After PCR amplification, the PCR product was purified by PCR purification kits (QIAquick; QIAgen, Valencia, CA) and diluted serially with distilled water. PCR product concentration and quality were measured with a Bio-Rad SmartSpec 3000 spectrophotometer. The serially diluted PCR products of tDNA were used as DNA samples for the experiments.

2.4. Synthesis of nanoparticles

Gold nanoparticles were synthesized using a previously published procedure (Zhang et al., 2009). Hydrogen tetrachloroaurate (III) trihydrate aqueous solution (1 mM, 50 mL) was heated with stirring on a hotplate. Once it refluxed vigorously, the solution was slowly titrated with 5 mL of 38.8 mM sodium citrate. The dimension and spectroscopic properties of AuNPs were characterized by a TEM and UV–vis-NIR scanning spectrophotometer. Nanoparticle tracers (PbS and CdS) were prepared according to the literature (Ding et al., 2009; Zhu et al., 2004) by using 3-mercaptoacetic acid as a stabilizer. Briefly, 3-mercaptoacetic acid (9.22 μL) was added to 50 mL of 0.4 mM $Pb(NO_3)_2$ solution; pH was adjusted to 7 with 0.5 M NaOH. The solution was bubbled with nitrogen for 30 min, then 1.34 mM Na_2S was dropwise added to the mixture. The reaction was carried out for 24 h under bubbled nitrogen, and then gradually a brown colloid was formed. For CdS nanoparticles, 2 μL of 3-mercaptoacetic acid was added to 100 mL of 1 mM $CdCl_2$ solution; pH was adjusted to 11 using 0.5 M NaOH. The solution was bubbled with nitrogen for 30 min, then 50 mL of 1.34 mM Na_2S was dropwise added. The reaction was carried out for 24 h under bubbled nitrogen, and a yel-

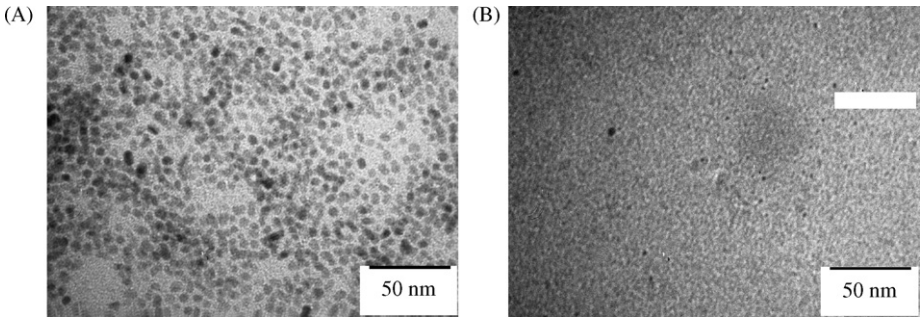

Fig. 1. TEM images of NTs: (A) CdS, showing an average diameter of 7 nm and (B) PbS, showing an average diameter of 3 nm.

lowish colloid was gradually formed. Both NTs were characterized using TEM.

2.5. Functionalization of nanoparticles

Functionalization of AuNPs with thiolated 1pDNA and bDNA, and functionalization of MNPs with 2pDNA through sulfo-SMCC were shown in our previous publication (Zhang et al., 2009). The thiolated oligonucleotide was suspended in 100 μL of 0.1 M DTT solution and the mixture was allowed to stand at room temperature for 2 h. Nap-5 columns were then used to purify the reduced thiolated oligonucleotides. The synthesized AuNPs (1 mL), purified thiolated bDNA (5 nmol), and purified thiolated 1pDNA (0.05 nmol) were then mixed together, comprising a 100:1 ratio of bDNA-to-1pDNA. Thiolated DNA would form a self-assembled monolayer on the surface of AuNPs. After a serial salt addition, the particles were stabilized for long-time storage at room temperature.

For the MNPs, the polyamine-functionalized iron oxide particles (1 mg) were reacted with 300 μg of sulfo-SMCC bifunctional linker for 2 h in 1 mL coupling buffer (0.1 M PBS buffer, 0.2 M NaCl, pH 7.2). After rinsing, the reduced thiolated 2pDNA (1 nmol) was added into 1 mL coupling buffer containing sulfo-SMCC-modified MNPs and reacted for 8 h. The functionalized MNPs were then suspended in 35 mL of 10 mM sulfo-NHS acetate. The solution was incubated and shaken at room temperature to block the unreacted sulfo-SMCC on the surface of MNPs. After passivation, the particles were centrifuged at 4000 rpm for 1 min and washed with passivation buffer (0.2 M Tris, pH 8.5) and then with a storage buffer (10 mM PBS buffer, 0.2 M NaCl, pH 7.4).

To conjugate NTs with bDNA on AuNPs, 1-ethyl-3-[3-dimethylaminopropyl] carbodiimide hydrochloride (EDC) and N-hydroxysuccinimide (NHS) were used to link the carboxylic group on NTs and amine group on bDNA. EDC (5 mg) was added to 25 μL NTs, then 50 μL of 9% NHS in dimethyl sulfoxide were added. Hydrochloride (775 μL, pH 5) was added immediately. The reaction was carried out on vortex at room temperature for 20 min. To keep the optimal pH value of the reaction, 5 μL of phosphate buffer (1 M $NaCO_3$, pH 8) were added. The solution was shaken for 8 h at room temperature and the conjugation solution was washed with water at 13,000 rpm 3 times before usage.

After conjugation, the two functionalized 1pDNA-AuNP-bDNA-NTs for *pagA* gene and for *Iel* gene were mixed in a 1:1 ratio. The two 2pDNA-coated MNPs were mixed in a 1:1 ratio also for the multiple detection. The nanoparticles then were ready for the bio-barcode assay.

2.6. Bio-barcode assay

A solution containing two tDNAs in one PCR tube was heated at 95 °C for 10 min to separate the dsDNA into ssDNA and then cooled rapidly at 4 °C. Serially diluted DNA samples (40 μL) were mixed with 0.8 mg MNP-2pDNA in 200 μL assay buffer (10 mM PBS buffer, 0.15 M NaCl, 0.1% SDS, pH 7.4). The hybridization reaction was maintained at a temperature of 45 °C for 1 h in an incubator. After hybridization, the MNP-2pDNA/tDNA was washed twice with the assay buffer, then resuspended in 200 μL assay buffer. Meanwhile, the functionalized 1pDNA-AuNP-bDNA-NTs complex was centrifuged at 13,000 rpm for 20 min and the unreacted thiolated oligonucleotides in the supernatant were removed. The purified 1pDNA-AuNP-bDNA-NTs complex was resuspended in 200 μL assay buffer, and 40 μL was then added into 200 μL solution containing the MNP-2pDNA/tDNA. The hybridization was incubated at 45 °C for 1 h with shaking. After the sandwich structure (MNP-2pDNA/tDNA/1pDNA-AuNP-bDNA-NTs) was formed, the solution was put on the magnetic separator for 3 min and then the super-

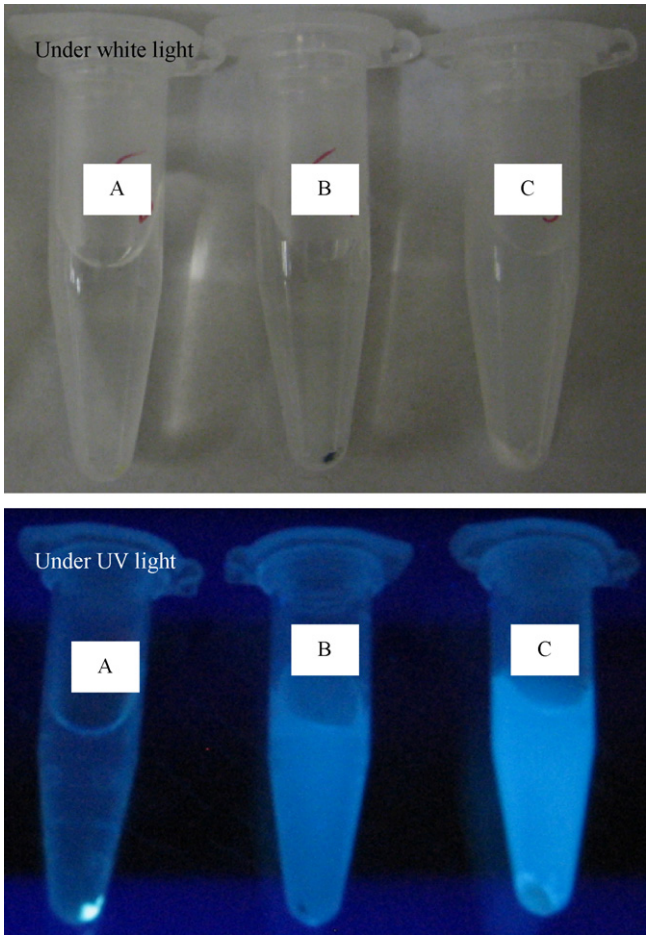

Fig. 2. Confirmation of conjugation of NTs and AuNPs.

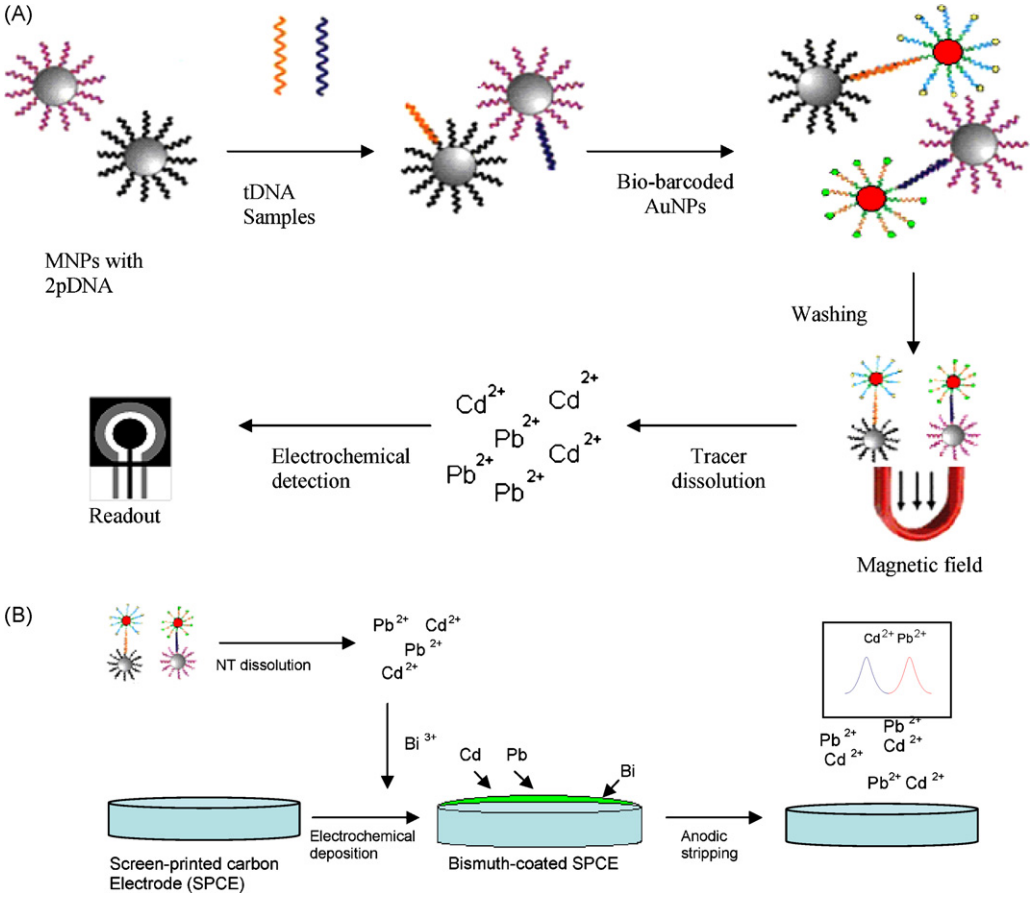

Fig. 3. Schematic of the multiple bio-barcode biosensor: (A) bio-barcode assay and (B) SWASV measurement.

natant was removed. The sandwich structures were washed five times with 500 μL of assay buffer in order to effectively remove the excess 1pDNA-AuNP-bDNA-NTs complex that was not specifically bound to the MNP-2pDNA/tDNA complex through hybridization. The washed sandwich structure was dissolved in 10 μL of 1 M nitric acid to release the NT ions (Pb^{2+} or Cd^{2+}). After addition of 90 μL of acetate buffer solution (0.1 M, pH 4.5) with 1 mg/L bismuth, the released NT ions were ready for electrochemical measurement. The attractive characteristic of bismuth is attributed to the formation of multi-component bismuth alloys with numerous heavy metals, such as Pb^{2+}, Cd^{2+}, and Zn^{2+}, while facilitating the electrodeposition of heavy metals.

2.7. Electrochemical analysis

Stripping voltammetric measurements were performed with an in situ deposition of the bismuth film and NT ions in the presence of dissolved oxygen. Studies were carried out by dropping a 100 μL of the sample solution in the well. A deposition potential of −1.2 V vs. Ag/AgCl was applied to the carbon working electrode without stirring the solution. After deposition, the voltammogram was recorded by applying a positive-going square-wave voltammetric potential scan (with a frequency of 20 Hz, amplitude of 25 mV, and potential step of 5 mV). The scan was from −1.2 V to 0.0 V (Wang et al., 2000). Based on our previous optimization studies, 1 mg/L of bismuth and 10 min of deposition time were used for all SWASV measurements. All experiments were carried out at room temperature. Every measurement was replicated three times. All curves were the average of three test results.

3. Results and discussion

3.1. Characterization of nanoparticles

The dimensions of the nanoparticles were characterized by using a TEM. Our previous result (Zhang et al., 2009) showed that the synthesized AuNPs had an average diameter of 15 nm. The absorption peak of the AuNPs was at 519 nm. Fig. 1 shows a TEM image of our synthesized CdS nanoparticles with an average diameter of 7 nm, and PbS nanoparticles with an average diameter of 3 nm. After 1 month of storage at 4 °C, the CdS and PbS NTs were stable and did not aggregate.

3.2. Functionalization of nanoparticles

Confirmation of the functionalization of MNPs and AuNPs was accomplished in our previous publication (Zhang et al., 2009). 1-Ethyl-3-[3-dimethylaminopropyl] carbodiimide hydrochloride (EDC) and N-hydroxysuccinimide (NHS) were used to crosslink the carboxylic group on NTs and the amine group on bio-barcoded AuNPs. Fig. 2 shows 3 test tubes labeled A, B, C after centrifugation at 13,000 rpm for 30 min. Tube A contains bio-barcoded AuNPs, NTs, EDC and NHS. Tube B and C are two controls. Tube B has no crosslinker while tube C only contains CdS NTs. There is a pellet that shows a yellowish fluorescence under UV light in tube A. After centrifugation, the conjugated particles became larger and were easier to precipitate. Most of the NTs were conjugated with AuNPs and were precipitated in the bottom. The precipitate shows a fluorescence signal under UV light (Fig. 2A). In tube B, there is a red pellet

under white light in the bottom, while the solution shows yellowish fluorescence under UV light. It shows that without crosslinkers, the NTs and bio-barcoded AuNPs cannot be conjugated. The AuNPs are larger and can be precipitated at 13,000 rpm so that we can see the red pellet under white light, while the NTs are smaller and still suspend in solution, showing fluorescence in the solution under UV light. Tube C shows that centrifugation does not precipitate the NTs. Overall, these results show that the conjugation of NTs to the bio-barcoded AuNPs has been successful.

3.3. Bio-barcode DNA assay amplification and detection

Fig. 3A is a schematic showing the multiple bio-barcode assay. After immobilization of oligonucleotides on the surface of nanoparticles, both nanoparticles bind to the tDNA to form a sandwich structure as a result of the specificity of pDNA. Before hybridization, two bio-barcoded AuNPs were mixed in a 1:1 ratio. One was PbS-AuNP-bDNA-1pDNA which recognizes the *pagA* gene from *B. anthracis*, and the other was CdS-AuNP-bDNA-1pDNA which recognizes the *Iel* gene of *S. enteritidis*. Then two 2pDNA coated MNPs were mixed in a 1:1 ratio also. One was specific to *pagA* gene from *B. anthracis* and the other was specific to *Iel* gene of *S. enteritidis*. When the tDNA samples hybridize with the pDNA on the MNPs, a MNP-2pDNA/tDNA complex (middle picture) is formed. Then the 1pDNA-AuNP-bDNA-NTs complex is added to form a sandwich structure consisting of MNP-2pDNA/tDNA/1pDNA-AuNP-bDNA-NTs. After hybridization is complete, the NTs on the bDNA are released in 1 M nitric acid and the NT ions are measured by SWASV on the SPCE chip. Fig. 3B shows SWASV measurements performed with an in situ deposition of bismuth film and target metals (Pb and Cd) in the presence of dissolved oxygen using a potentiostat/galvanostat.

Fig. 4 shows the electrochemical signal of anodic oxidation of Pb from *pagA* gene from *B. anthracis* during a single target detection. The peak current of various tDNA concentrations (2 ng/mL, 0.2 ng/mL, 20 pg/mL, 2 pg/mL, 0.2 pg/mL, 0.02 pg/mL, and 2 fg/mL) are 96 μA, 76 μA, 63 μA, 46 μA, 21 μA, 14 μA, and 13 μA, respectively. The peak current of various tDNA concentrations increased with increasing concentration. The shift of peak potential is noticeable. There could be two reasons. First, the reference potential on Ag/AgCl on two-electrode system could change with the current which flows through the circuit. Second, the SPCEs we used for measurement are not exactly identical. The base line is around 7 μA. At tDNA concentration of 0.2 pg/mL, the ratio of signal to noise (S/N) is equal to 3. Therefore, the biosensor sensitivity for single detection of *pagA* gene from *B. anthracis* is 0.2 pg/mL or 200 fg/mL.

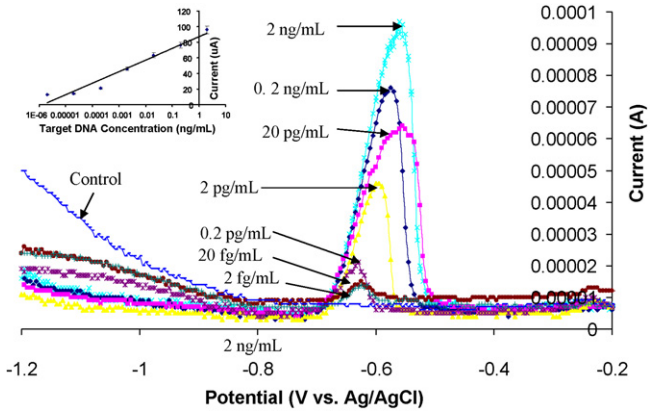

Fig. 4. Single detection of the bio-barcode biosensor using PbS NTs. The inset shows the relationship of tDNA concentration and peak current.

Fig. 5 shows the electrochemical signal of anodic oxidation of Pb and Cd, and the specificity of the biosensor. When the sample contains no tDNA, there are no stripping signal at −0.61 V (Pb) and −0.87 V (Cd). When the sample contains 0.05 μg/mL of the *pagA* gene from *B. anthracis* and the insertion element (*Iel*) gene of *S.*

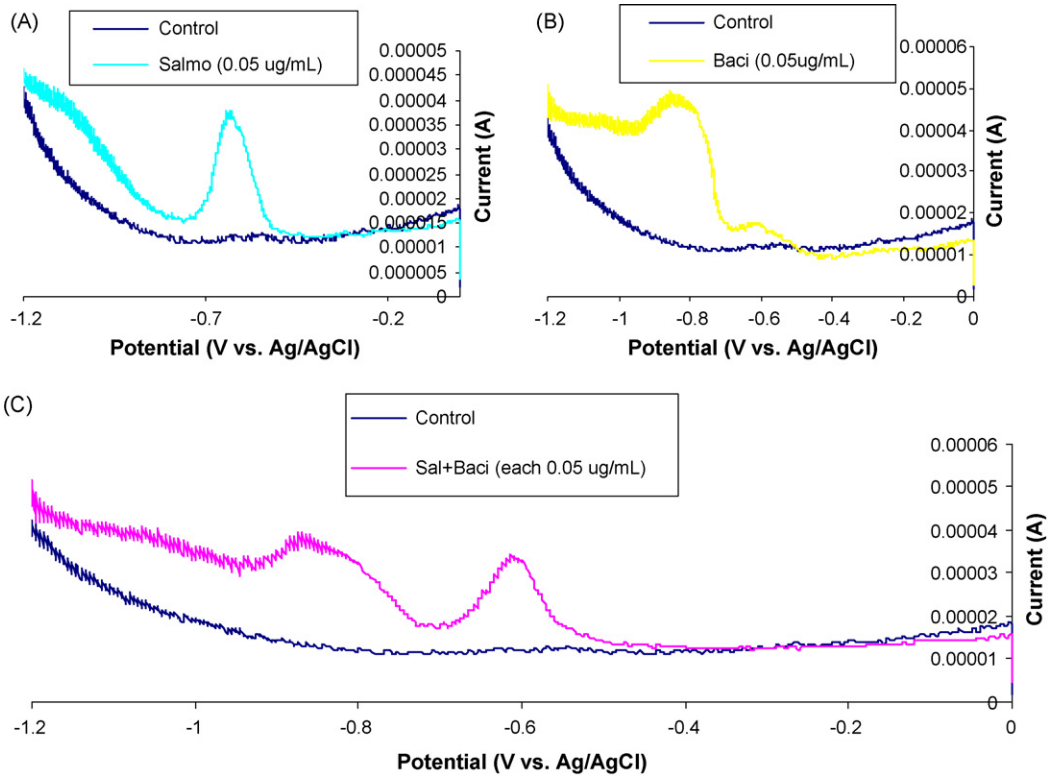

Fig. 5. Specificity test of the multiple bio-barcode biosensor.

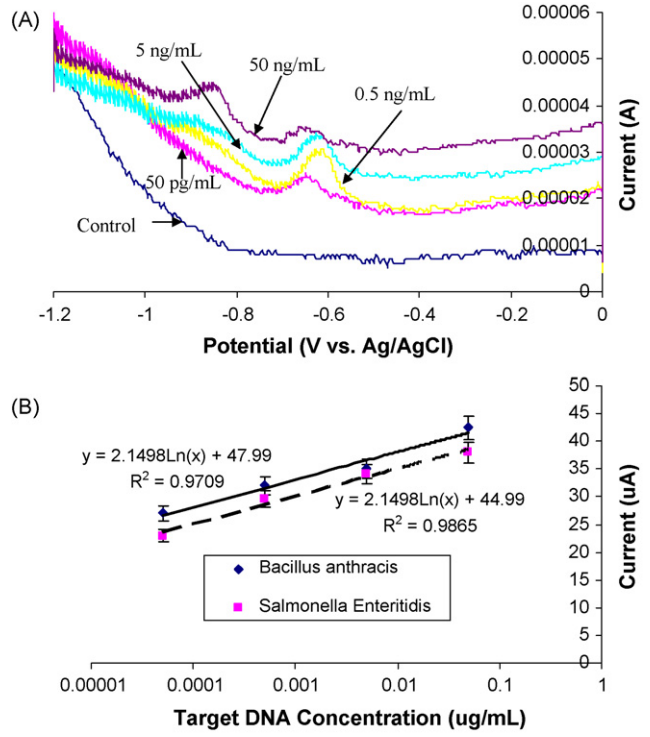

Fig. 6. The stripping signal of released NT ions (Pb^{2+} and Cd^{2+}) with different concentrations of tDNAs: (A) stripping voltammogram and (B) the calibration plot between peak current and the tDNA concentration.

enteritidis, the peak current at −0.61 V (vs. Ag/AgCl) is 35 μA and the peak current at −0.87 V (vs. Ag/AgCl) is 39 μA, respectively. When there is only 0.05 μg/mL of *pagA* gene from *B. anthracis*, the stripping voltammogram shows a current peak of 39 μA at −0.61 V from the anodic oxidation of Pb, and no peak at −0.87 V. When there is only 0.05 μg/mL of the insertion element (*Iel*) gene of *S. enteritidis*, the stripping voltammogram shows a current peak of 46 μA at −0.87 V from the anodic oxidation of Cd, and a small peak at −0.61 V. The possible reason would be that the washing steps were not thorough and the unreacted PbS NTs generated the noise. Overall, these results show that this bio-barcoded DNA sensor has a good specificity. It can differentiate *pagA* gene from *B. anthracis* (labeled with CdS) and *Iel* gene of *S. enteritidis* (labeled with PbS) when the concentration of tDNA is relatively high.

Fig. 6 shows the sensitivity of the biosensor. For the detection of the *pagA* gene from *B. anthracis*, the peak currents at −0.61 V (vs. Ag/AgCl) of various concentrations (50 ng/mL, 5 ng/mL, 500 pg/mL, and 50 pg/mL) are 38 μA, 34 μA, 29.5 μA, and 23 μA, respectively. For the detection of the insertion element (*Iel*) gene of *S. enteritidis*, peak currents at −0.87 V at various tDNA concentrations (50 ng/mL, 5 ng/mL, 500 pg/mL, and 50 pg/mL) are 42.5 μA and 35 μA, 32 μA, and 27 μA, respectively. Fig. 6B shows that the stripping signals of released Pb^{2+} and Cd^{2+} have a linear relationship with the logarithmic concentrations of target DNA, that is, the signal increases with increasing logarithmical concentration of target DNA. Compared to the single detection with PbS NTs in Fig. 4, Fig. 6 shows a lower peak current value with higher concentration. The presence of residual materials in a multiple detection assay is obviously influencing the deposition and/or reduction of the lead ions.

The base line at −0.61 V and −0.87 V are 7 μA and 10 μA, respectively. Considering the ratio of signal-to-noise (S/N) > 3, the results show that the detection limits of this bio-barcoded DNA sensor are as low as 0.5 ng/mL of the insertion element (*Iel*) gene of *S. enteritidis* using CdS, and 50 pg/mL of *pagA* gene from *B. anthracis* using PbS NTs.

4. Conclusion

A highly amplified, nanoparticle-based, bio-barcoded electrochemical biosensor for the multiple detection of *pagA* gene (accession number, M22589) from *B. anthracis* and insertion element (*Iel*) gene (accession number, Z83734) from *S. enteritidis* has been described in this paper. The biosensor system is mainly composed of three nanoparticles: gold nanoparticles (AuNPs), magnetic nanoparticles (MNPs), and nanoparticle tracers (NTs, such as PbS and CdS). AuNPs, PbS and CdS nanoparticles were synthesized by chemical methods and characterized by TEM. The conjugation of carboxylic group on NTs and amine group on bio-barcoded AuNPs was efficient. After mixing the nanoparticles with the tDNA, the sandwich structure (MNP-2pDNA/tDNA/1pDNA-AuNP-bDNA-NTs) was formed. The electrochemical signal of released NT ions increased with increasing tDNA concentration. The results show that the biosensor has a good specificity, and the sensitivity of single detection of *pagA* gene from *B. anthracis* using PbS NTs is as low as 0.2 pg/mL. The detection limits of this multiplex bio-barcoded DNA sensor are as low as 0.5 ng/mL of the insertion element (*Iel*) gene of *S. enteritidis* using CdS, and 50 pg/mL of *pagA* gene from *B. anthracis* using PbS NTs. The nanoparticle-based bio-barcoded DNA sensor has potential applications in multiple detection of bioterrorism threat agents, co-infection, and multiple contaminants in the same sample.

Acknowledgments

This publication was developed under DHS Science and Technology Assistance Agreement No. DHS-2007-ST-061-000003 awarded by the U.S. Department of Homeland Security. It has not been formally reviewed by DHS. The views and conclusions contained in this document are those of the authors and should not be interpreted as necessarily representing the official policies, either expressed or implied, of the U.S. Department of Homeland Security. The Department of Homeland Security does not endorse any products or commercial services mentioned in this publication.

The authors wish to acknowledge the Center for Advanced Microscopy at Michigan State University for the TEM image support.

References

Ding, C., Zhang, Q., Lin, J.-M., Zhang, S.-S., 2009. Biosens. Bioelectron. 24 (10), 3140–3143.
Drummond, T.G., Hill, M.G., Barton, J.K., 2003. Nat. Biotechnol. 21 (10), 1192–1199.
Dubertret, B., 2005. Nat. Mater. 4 (11), 797–798.
Goluch, E.D., Nam, J.M., Georganopoulou, D.G., Chiesl, T.N., Shaikh, K.A., Ryu, K.S., Barron, A.E., Mirkin, C.A., Liu, C., 2006. Lab Chip 6 (10), 1293–1299.
Hill, H.D., Mirkin, C.A., 2006. Nat. Protoc. 1 (1), 324–336.
Huang, G.S., Wang, M.T., Hong, M.Y., 2006. Analyst 131 (3), 382–387.
Jackson, N.M., Hill, M.G., 2001. Curr. Opin. Chem. Biol. 5 (2), 209–215.
Karadeniz, H., Gulmez, B., Sahinci, F., Erdem, A., Kaya, G.I., Unver, N., Kivcak, B., Ozsoz, M., 2003. J. Pharm. Biomed. Anal. 33 (2), 295–302.
Li, B., Du, Y., Dong, S., 2009. Anal. Chim. Acta 644 (1–2), 78–82.
Mathew, F.P., Alocilja, E.C., 2005. Biosens. Bioelectron. 20 (8), 1656–1661 (Special issue).
Fojta, M., Havran, L., Billova, S., Kostecka, P., Masarik, M., Kizek, R., 2003. Electroanalysis 15 (5–6), 431–440.
Nam, J.M., Stoeva, S.I., Mirkin, C.A., 2004. J. Am. Chem. Soc. 126 (19), 5932–5933.
Ozkan-Ariksoysal, D., Tezcanli, B., Kosova, B., Ozsoz, M., 2008. Anal. Chem. 80 (3), 588–596.
Pal, S., Ying, W., Alocilja, E.C., Downes, F.P., 2008. Biosyst. Eng. 99 (4), 461–468.
Poonam, P., Deo, N., 2008. Sens. Actuators B: Chem. 135 (1), 327–335.
Pu, K.-Y., Pan, S.Y.-H., Liu, B., 2008. J. Phys. Chem. B 112 (31), 9295–9300.
Ricci, F., Zari, N., Caprio, F., Recine, S., Amine, A., Moscone, D., Palleschi, G., Plaxco, K.W., 2009. Bioelectrochemistry 76 (1–2), 208–213.
Sassolas, A., Leca-Bouvier, B.D., Blum, L.J., 2008. Chem. Rev. 108 (1), 109–139.
Song, L., Ahn, S., Walt, D.R., 2005. Emerg. Infect. Dis. 11 (10), 1629–1632.
Steel, A.B., Herne, T.M., Tarlov, M.J., 1998. Anal. Chem. 70 (22), 4670–4677.
Templin, M.F., Stoll, D., Schrenk, M., Traub, P.C., Vohringer, C.F., Joos, T.O., 2002. Trends Biotechnol. 20 (4), 160–166.
Wang, J., 2002. TrAC Trends Anal. Chem. 21 (4), 226–232.

Wang, J., Liu, G., Merkoci, A., 2003. J. Am. Chem. Soc. 125 (11), 3214–3215.
Wang, J., Lu, J., Hocevar, S.B., Farias, P.A., Ogorevc, B., 2000. Anal. Chem. 72 (14), 3218–3222.
Wang, J., Zhang, S., Zhang, Y., 2010. Anal. Biochem. 396 (2), 304–309.
Wang, S.J., Yeh, D.B., 2002. Lett. Appl. Microbiol. 34 (6), 422–427.
Weng, J., Zhang, J., Li, H., Sun, L., Lin, C., Zhang, Q., 2008. Anal. Chem. 80 (18), 7075–7083.
Yang, I.V., Thorp, H.H., 2001. Anal. Chem. 73 (21), 5316–5322.
Zhang, D., Alocilja, E.C., 2008. IEEE Sens. J. 8 (6), 775–780.
Zhang, D., Carr, D.J., Alocilja, E.C., 2009. Biosens. Bioelectron. 24 (5), 1377–1381.
Zhu, N., Zhang, A., Wang, Q., He, P., Fang, Y., 2004. Electroanalysis 16 (7), 577–582.